Surface Plasmon Resonance Imaging (SPR*i*) in Combination with Machine Learning for Microarray Analysis of Multiple Sclerosis Biomarkers in Whole Serum

Alexander S. Malinick, Daniel D. Stuart, Alexander S. Lambert, and Quan Cheng*

Department of Chemistry, University of California, Riverside, CA 92521, USA

*Corresponding author: Quan Cheng

Tel: (951) 827-2702, Fax: (951) 827-4713

Email: quan.cheng@ucr.edu

Graphic Content

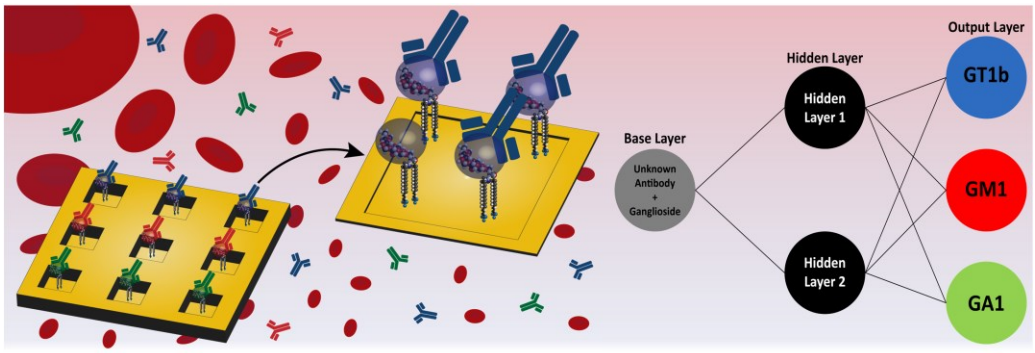

Abstract:

Multiple sclerosis (MS) is the most common autoimmune disease observed in young adults and is known to be exceptionally difficult to diagnose accurately. Current diagnostic methods are considered unreliable and inefficient, and they typically lack the needed specificity that allows for routine monitoring of disease progression. In this work, we report a surface plasmon resonance imaging (SPRi) method in combination with carbohydrate microarrays for the detection of multiple sclerosis biomarkers in undiluted serum. A working range of 1 to 100 ng/mL was demonstrated with the limit of detection (LODs) below 7 ng/mL. The microarrays utilized in this work were coated with perfluorodecyltrichlorosilane (PFDTS) to interact strongly with the hydrophobic tails of the ganglioside antigens, allowing for desirable antigenic display in a manner mimicking a myelin sheath. Machine learning (ML) algorithms were applied to the carbohydrate array/SPRi data analysis to understand and characterize the cross reactivities observed between the antibodies. Both endpoint results and SPRi sensorgrams were analyzed with statistical models for the evaluation of binding events that include kinetic and steady state components. In addition, K-nearest neighbor (knn) and neural net (nnet) were utilized to examine specific and cross-reactive binding, yielding higher accuracy than what traditional methods can achieve. The combination of ML models and microarray data provides a comprehensive understanding of complex interactions and could be used to differentiate and identify closely behaving biomarkers in a clinical setting.

Key Words: Surface plasmon resonance imaging, biomarker, ganglioside, microarray, machine learning, multiple sclerosis

INTRODUCTION:

Rapid detection and monitoring of disease biomarker levels is vital to medical diagnosis and therapeutic intervention, and thus constitutes an important part of research endeavors for the advancement of medical sciences.(Broza et al., 2019) These biomarkers allow for early diagnosis and thus enable disease differentiation, leading to faster implementation of treatments and targeted therapies.(Clark and Kodadek, 2016) For multiple sclerosis (MS), several antibody and protein biomarkers were found to target cell membrane components of the myelin sheath, such as gangliosides and sulfatides. The myelin sheath is a lipid rich substance that surrounds and insulates the neurons of the central nervous system (CNS), allowing for transmission of electrical pulses that control various functions throughout the body.(Graner et al., 2020; Kuerten et al., 2020; Mizutani et al., 2001; Pender et al., 2003) Among various membrane components of the myelin sheath, gangliosides have received extensive research attention as they are significant for maintaining structural stability, assist in cell to cell interactions, and aid in the regeneration and growth of axons.(Cawley et al., 2021; Nowack et al., 2021; Schnaar, 2010) It has been observed that with the progression of MS, the myelin sheath's integrity diminishes, severely impacting the CNS' ability to communicate with the rest of the body.(Ivanova and Zakharova, 2017) The damaged neural areas will cease to function normally, resulting in the symptoms associated with MS.(Höftberger et al., 2020)

Current diagnosis of MS relies heavily on characterizing damage to the CNS by scanning for plaques or scar tissue, which indicate that trauma or an autoimmune attack has occurred.(Ghasemi et al., 2017; Shedko et al., 2020) Evaluation of the severity of the plaques is normally achieved by using a combination of several techniques, including magnetic resonance imaging (MRI), evoked potential, spinal taps, and blood tests,(Ghasemi et al., 2017) while only spinal taps are routinely used for direct detection of MS protein biomarkers.(Shedko et al., 2020) Collection of cerebrospinal fluid (CSF), however, requires the use of lumbar punctures, which are incredibly painful, difficult to perform, and only allow for a small amount of CSF to be collected,(Costerus et al., 2018) leading to some diminished interest in the monitoring of MS progression.(Derkus et al., 2017) Concurrently, there has been a great deal of interest in the development of new approaches for quantifying MS biomarkers in blood.(Lycke and Zetterberg, 2017) Presently, blood tests are routinely performed to screen for established markers of other

diseases that have similar symptoms as MS for the purpose to rule them out in diagnosis.(Brownlee et al., 2017) They are not normally used for direct MS diagnosis due to limited biomarker presence in the blood resulting in much lower concentrations when compared to CSF samples.(Ziemssen et al., 2019) Therefore, moving to a blood-test based detection method for MS markers would require technical development for sensitivity improvement and robustness that could 1) quantify concentrations and analyte/antigen interactions concurrently, 2) identify and differentiate cross reactivity between biomarkers, and 3) eliminate background signals from various other components in the patients' blood sample.

While fluorescence and chemiluminescence detection schemes have been used,(Yang et al., 2020) surface plasmon resonance imaging (SPRi), a label-free, real time, and direct detection method, has increasingly been used broadly to detect disease biomarkers in various biological samples.(Sharafeldin and Davis, 2021) The benefits offered by SPRi includes compatibility with microarrays that allow for screening of multiple biomarkers simultaneously in a high throughput and multiplexed manner, which can drastically improve the monitoring of disease progression.(Lambert et al., 2018; Malinick, A. S. et al., 2020) A major drawback, however, is the nonspecific binding when dealing with complex samples, such as blood.(Sharafeldin and Davis, 2021) Another challenge is the cross reactivity among various biomarkers in the sample, which is a particularly troublesome issue for anti-ganglioside antibody detection where the difference among carbohydrate headgroups is small. This convolutes signals and makes detection unreliable due to false positive and/or negative results, causing major concerns for use in clinical studies.(Mescheriakova et al., 2018) Antifouling surfaces and new SPRi methodologies have therefore been the focus of many works to reduce these undesirable interferences.(D'Agata et al., 2021; Damodaran and Murthy, 2016; Lambert et al., 2020; Malinick, A. S. et al., 2020; Nair et al., 2020; Rikkert et al., 2020; Wu et al., 2021; Yang et al., 2020)

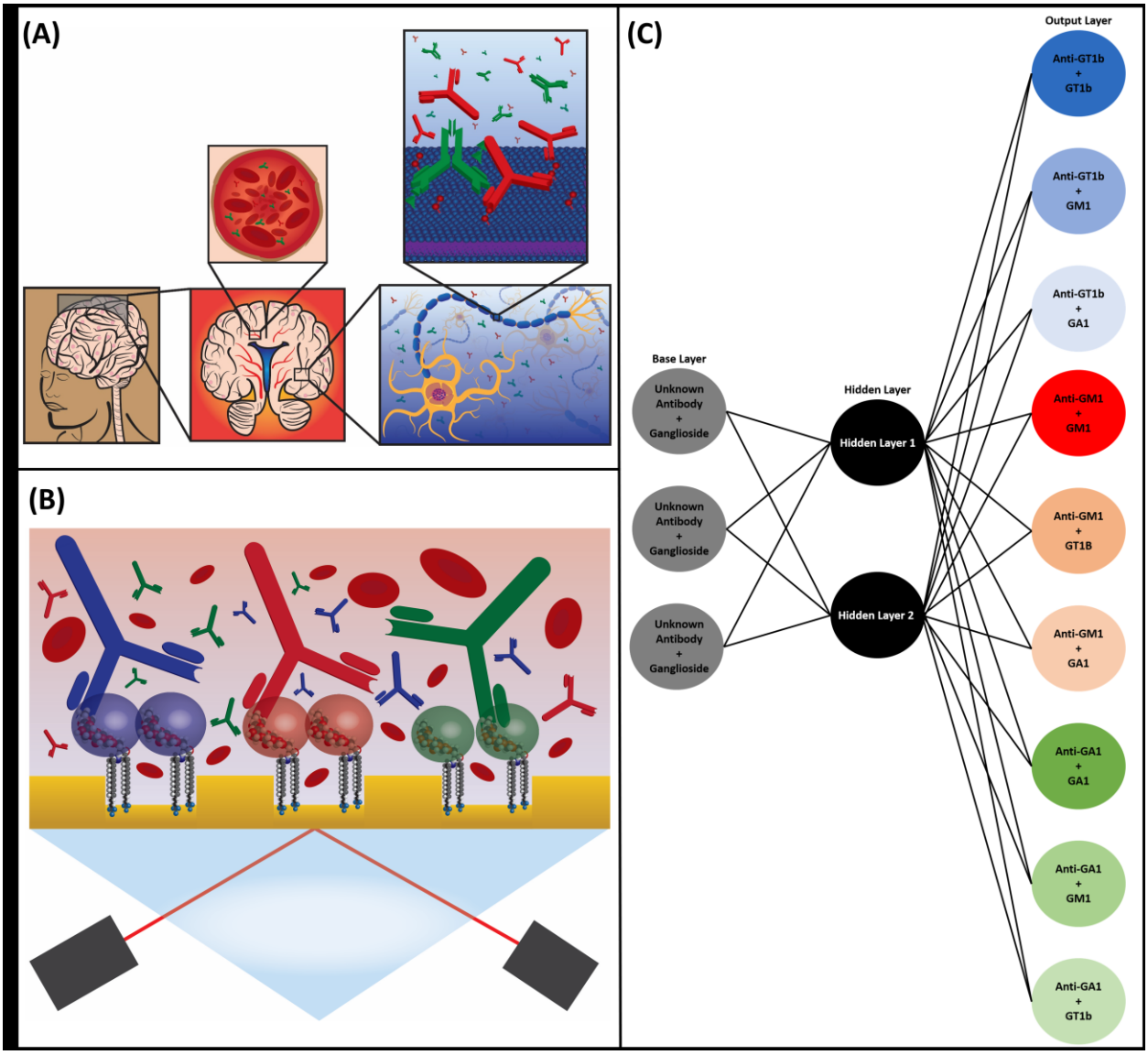

Scheme 1. (A) Graphical representation of the biological process of antibodies attacking the myelin sheath in multiple sclerosis during an autoimmune attack. (B) Capture and detection scheme of anti- ganglioside antibodies associated with multiple sclerosis via the ganglioside microarray and SPRi. (C) Visualization of the machine learning algorithm for a neural network process including base layer, hidden layers, and output layers for all potential analyte antigen interaction in this study.

Recently we reported a near super hydrophobic, perfluorodecyl-trichlorosilane (PFDTS) surface for the detection of MS biomarkers. The antifouling properties of the ganglioside PFDTS substrate were evaluated and characterized, and detection of 3 anti-ganglioside antibodies in 10 % serum was successfully demonstrated.(Malinick, A. S. et al., 2020) In this work we expand the study to investigate the sensing performance in clinical conditions by coupling machine learning to the differentiation of MS specific antibodies in undiluted serum (Scheme 1). Extensive controls were used to evaluate cross reactivity between the investigated antibodies and gangliosides, which is critical for obtaining an accurate diagnosis in a clinical setting. To assess cross reactivity among structurally similar carbohydrate antigens, we have performed modeling and statistical analysis using various machine learning (ML) algorithms for post-acquisition data analysis. Data sets of endpoint results, association, steady state, and dissociation energies were utilized, which provided a more comprehensive understanding into the observed interactions than what traditional methods can achieve.(Cui et al., 2020) Categorization by ML relies on complex algorithms to detect patterns in the raw data where similar observations can be grouped or clustered together.(Das et al., 2015b) This in-depth analysis allows for the discovery of previously overlooked patterns that can be used to train the ML models to aid in the identification and differentiation of analytes present in a complex biological sample.(Volk et al., 2020) The findings of the presented study establishes a new methodology to address the technical difficulties of identifying analyte/antigen interactions in complex media and that by correctly training ML models, they can be implemented to improve biomarker detection for disease diagnosis.

EXPERIMENTAL METHODS:

Materials and Reagents:

Monosialoganglioside GM_1 was purchased from Matreya (Pleasant Gap, PA). Trisialoganglioside GT_{1b} was obtained from Biosynth (Itsaca, Il). Asialoganglioside GA_1 was acquired from Sigma-Aldrich (St. Louis, MO). *1H,1H,2H,2H*-Perfluorodecyltrichlorosilane (PFDTS) was purchased from Fisher Scientific (Pittsburgh, PA). Anti asialoganglioside GA_1 human anti mouse monoclonal antibody and anti monoganglioside GM_1 rabbit polyclonal antibody, were both obtained from Abcam (Cambridge, UK). Anti Trisialoganglioside GT_{1b} ganglioside mouse monoclonal antibody

was obtained from Millipore Sigma (Billerica, MA). Human serum was purchased from Innovative Research (Upper Marlboro, MD).

Fabrication of SPRi Substrates:

The SPRi arrays biochips were fabricated via the protocol reported in a previous paper.(Abbas et al., 2011) In short, glass slides were spin-coated with hexamethyldisilazane (HMDS) to promote adhesion. After baking at 110 °C for approximately 1 minute, UV exposure via a Karl-Suss MA-6 system allowed for the creation of an array pattern on the photoresist, after which standard photoresist development protocols were implemented. A 2 nm layer of titanium was first deposited to act as an adhesion layer, after which a layer of 200 nm of gold was deposited to form wells. The remaining photoresist was removed from the surface with acetone. A second 2nm layer of titanium was deposited followed by a 48 nm layer of gold to form the sensing surface inside of the wells. PECVD was then used to deposit 1-3 nm of SiO_2 on the microarray chips, which would later be treated with PFDTS. The final product was a microarray consisting of 10x10 well arrays that were 200 nm deep and 600 μm in diameter.

Surface Functionalization and Preparation:

Functionalization of the chips was carried out with a similar protocol used previously.(Malinick, A. S. et al., 2020) The surface of the chips was submerged in 1 mM PFDTS in toluene. After 30 minutes, the chip was removed from the solution and rinsed with toluene, ethanol, and deionized water and dried under nitrogen gas. Once the chips were completely dry, 1.5 μL of the 100 μg/mL stock solution for each ganglioside was incubated and allowed to dry in air to create four different working channels. An S-shaped PDMS flow cell was used to create eight working wells per channel where functionalization and interactions occurred under the same configuration for reproducibility. The first channel was left un-functionalized as an internal reference to measure chip to chip variation, whereas 1.5 μL of 100 μg/mL stock solutions was employed for generating ganglioside channels with GA_1, GM_1, and GT_{1b}.

SPRi analysis:

SPRi measurements were conducted on a home-built setup; a detailed description of which can be found in previous work.(Wilkop et al., 2004) The functionalized chips were mounted onto an

optical stage that houses a PDMS flow cell. The array was placed in contact with an equilateral SF2 prism (n = 1.65) with a layer of refractive index matching fluid (Cargill Laboratories, Cedar Grove, NJ). A 648 nm light emitting diode (LED) was used as the light source for SPR excitation. Reflected images of the microarray were captured by a cooled 12-bit CCD camera (QImaging Retiga 1300) and data acquisition was controlled via a home built LabView program. Intensity data was normalized by using the intensity from the *p*-polarized light over the *s*-polarized beam and described as a percentage.

Statistical analysis and Machine Learning:

Partial least squares discrimination analysis (PLS-DA) plots were produced with MetaboAnalyst. Principal component analysis (PCA) was completed with the prcomp function in R and graphed with the ggbiplot package with an ellipse probability set to 95 % using the endpoint data. Neural Network (nnet) was used to analyze both the endpoint data and SPRi sensorgram data. Nnet was conducted using the nnet package for R and was plotted using an expanded grid in R. K nearest neighbor (Knn) from the caret package was used to evaluate regions of the sensorgram related to the antibody spiked in whole serum interaction study. The Knn model was visualized with ggbiplot packages. For ML 70 % of the data was used to train the models and 30 % to test. Each model had random iterations incorporated into them so that all of the data could be used to test the success of the model.

RESULTS AND DISCUSSION:

SPR imaging analysis of anti-gangliosides in Serum

Microarrays offer the benefit of detecting many biomarkers simultaneously. However, reliably and effectively using microarrays in a clinical setting requires an in-depth understanding of background signals from the biological sample and the cross reactivity between the biomarkers of interest that could be present in the sample.(D'Agata et al., 2021; Masson, 2017) The microarray used in this study has a 4 x 8 arrangement with the 3D printed looped flow cell, capable of monitoring the presence of many biomarkers concurrently. Previously, we showed that our myelin sheath mimic is capable of detecting and differentiating MS specific antibodies in diluted serum

at 100 ng/mL.(Malinick, A. S. et al., 2020) In this study, we expand the investigation and focus on detecting and differentiating three MS specific anti-ganglioside antibodies in whole serum at disease-relevant concentrations ranging from 3 to 25 ng/mL.(Ivanova and Zakharova, 2017) Antibodies for GT_{1b}, GM_1, and GA_1 gangliosides were used as they have been associated with symptoms commonly observed in MS.(Ivanova and Zakharova, 2017; Kuerten et al., 2020; Wanleenuwat and Iwanowski, 2019) Anti-GT_{1b} has been linked to the loss of muscle control in the limbs, whereas anti-GM_1 and anti-GA_1 are believed to play significant roles in the damage of myelin associated with the optic nerves, as they both have been correlated to changes in and loss of vision.(Hogan et al., 2013; Ivanova and Zakharova, 2017; Kappler and Hennet, 2020; Wanleenuwat and Iwanowski, 2019) Detection of these antibodies, as well as other anti-ganglioside antibodies, should drastically increase the confidence and speed at which a diagnosis is determined when coupled with currently established MS detection methods.

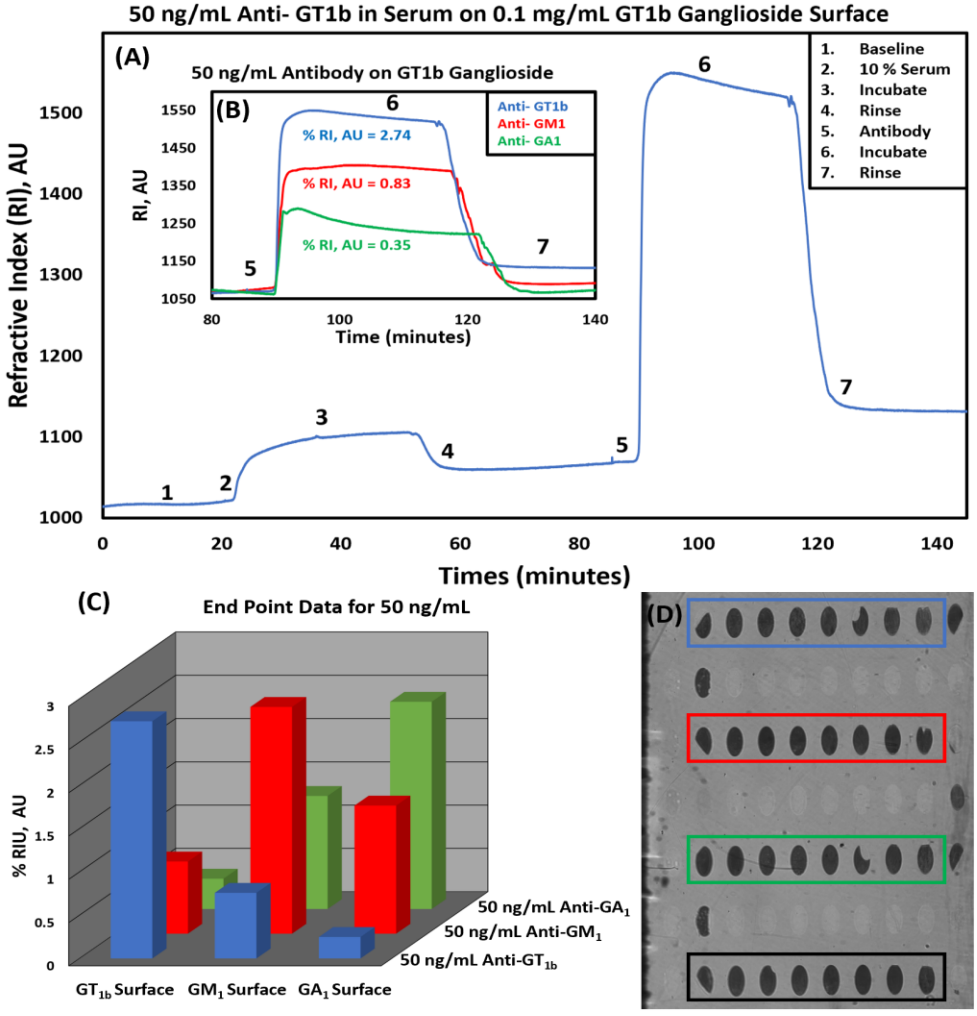

Figure 1. (A) Entire sensorgram for 50 ng/mL of anti-$GT1_b$ in serum on a $GT1_b$ ganglioside surface. (B) Average of 5 sensorgrams to depict association, steady state, and dissociation binding interactions for 50 ng/mL anti-$GT1_b$ (Blue), anti-GM_1 (Red), anti-GA_1 (Green) interacting with a $GT1_b$ ganglioside surface. (C) Average of all observed bulk changes caused by MS specific antibodies at 50 ng/mL in serum on the PFDTS functionalized ganglioside microarray. (Blue) % RI, AU caused by 50 ng/mL anti-GT_{1b} on 0.1 mg/mL GT_{1b}, GM_1, and GA_1 ganglioside surfaces, (Red) binding between 50 ng/mL anti-GM_1 and 0.1 mg/mL on a GT_{1b}, GM_1, and GA_1 ganglioside surfaces, and (Green) binding between 100 ng/mL anti-GA_1 and 0.1 mg/mL GT_{1b}, GM_1, and GA_1 ganglioside surfaces. (D) Image of ganglioside microarray by the CCD camera used in the SPR imaging experiments. Each color indicates the functionalization of the surface PFDTS only (Black), GA_1 ganglioside surface (Green), GM_1 ganglioside surfaces (Red), and GT_{1b} ganglioside surfaces (Blue).

Figure 1 shows the SPRi results for specific anti-gangliosides antibodies under various conditions and the microarray image by gangliosides. The first step in the experiment was to inject 10 % serum diluted with PBS to block the surface to account for cross reactivity and nonspecific binding. Different concentrations of serum dilutions were tested, but higher concentrations did not offer any benefits over the 10 % dilution. As shown in Figure 1 A and B, there is a large angle shift due to the change in refractive index units (RIU) once the spiked whole serum is introduced. This shift can be attributed to the high concentration of proteins and other biological components present in the sample.(Masson, 2017) Once the rinse cycle is initiated, the vast majority of the material that caused the large shift is rinsed off, leaving behind only the specific antibody/ganglioside interaction of interest and other materials of extremely high affinity. To confirm the specific interaction, we conducted cross reactivity evaluations with several antibodies for each concentration to determine how much of the observed shifts were due to specific analyte/antigen interactions, as shown in Figure 1B. The small amount of nonspecific binding can be attributed to the unique properties of the near super hydrophobic surface and the selectivity of the sialic acids (SA) present on the antigenic sensing sites of the gangliosides.(Malinick, A. S. et al., 2020) Figure 1C shows the bulk changes (in % RIU) of the investigated antibodies at 50 ng/mL with the ganglioside microarray. High cross reactivity can be observed between anti-GM_1 and anti-GA_1 and their respective gangliosides, whereas there is negligible cross reactivity between anti-GT_{1b} and anti-GA_1. This observation can be attributed to the number of SA for each

ganglioside.(Malinick, A. S. et al., 2020) This trend was present in all of the investigated concentrations and can be seen in the supporting information, Figures 2S (A-I). The PFDTS carbohydrate chips used here appear effective in addressing large levels of nonspecific binding from complex media and cross reactivity between analytes, one of the major challenges of label-free detection methods.(Masson, 2017)

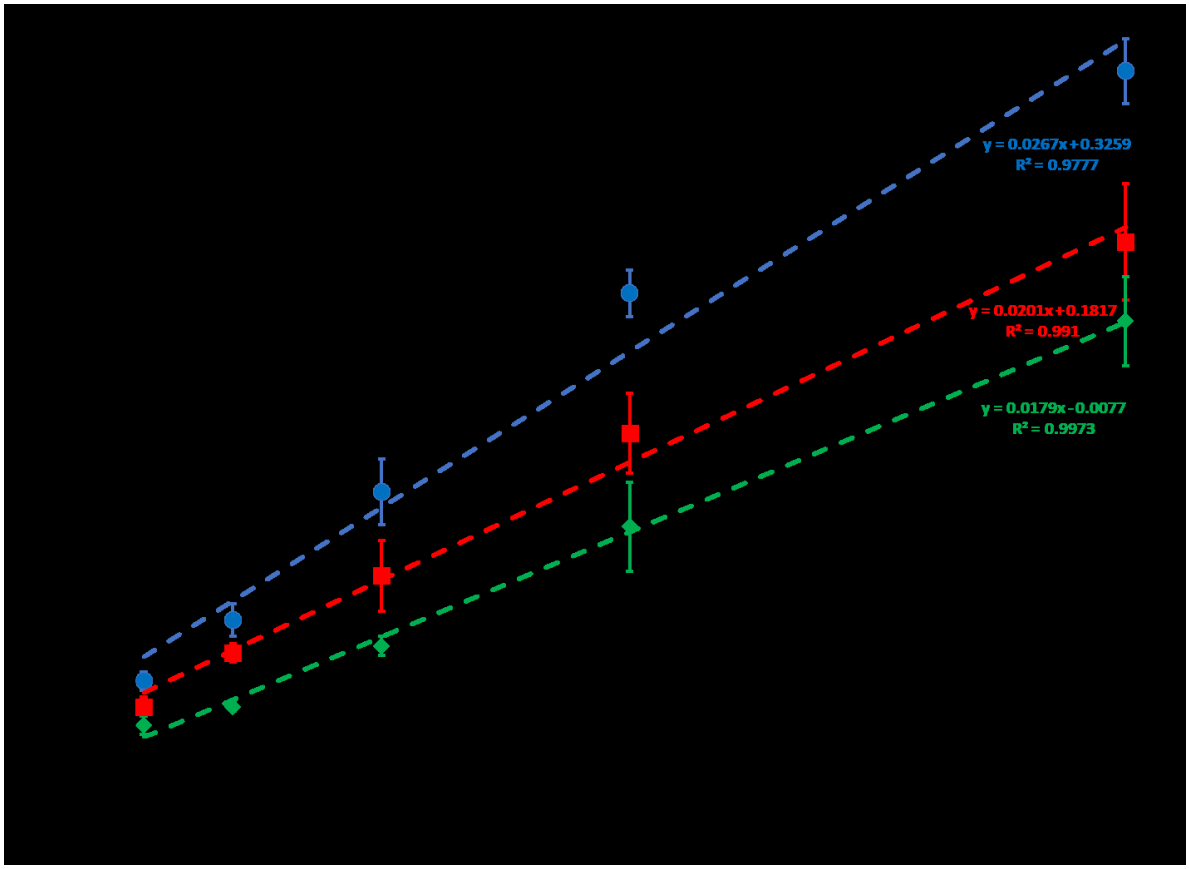

Figure 2. Calibration curve for the specific binding of all of the investigated antibodies in serum. Anti-$GT1_b$ (Blue), anti-GM_1 (Red), and anti-GA_1 (Green). Each data point is the average of at least 5 wells.

A calibration curve for anti-GT_{1b}, anti-GM_1, and anti-GA_1 after background subtraction is shown in Figure 2. Each surface has a working range of 1 ng/mL to 100 ng/mL in undiluted serum. The limits of detection (LOD) using the 3σ method were calculated to be 4.5 ng/mL, 5.6 ng/mL, and 6.6 ng/mL for anti-GT_{1b}, anti-GM_1, and anti-GA_1 respectively. Based on these calculations, the detection limit of the carbohydrate microarrays appears to fall within the concentration range

of antibodies typically seen in patient serum samples,(Häusser-Kinzel and Weber, 2019; Ziemssen et al., 2019) demonstrating that our microarray is capable of detecting, quantifying, and differentiating MS biomarkers in a clinical setting. These capabilities validate that our presented methodology offers unique and clear benefits when compared to other recently developed detection methods for MS specific biomarkers, as presented in Table 1. While each of the listed techniques have aided in the progression towards a more reliable and/or direct method for detecting and monitoring MS specific biomarkers, they all lack in one or several of the key capabilities that our method provides. Most notably in regards to the abilities to simultaneously screen, quantify, and differentiate multiple biomarkers in biological samples.

Table 1. Comparison of recent biosensors developed for the detection and monitoring of MS biomarkers.

Biomarker	**Bioreceptor**	**Method**	**Amplification**	**LOD**	**Detected in Biological Sample**	**Reference**
anti-GT_{1b} anti-GM_1 anti-GA_1	GT_{1b} ganglioside GM_1 ganglioside GA_1 ganglioside	SPRi	No	4.5 ng/mL or 30 pM 5.6 ng/mL or 37 pM 6.6 ng/mL or 44 pM	Yes whole serum	This work
anti-GT_{1b} anti-GM_1 anti-GA_1	GT_{1b} ganglioside GM_1 ganglioside GA_1 ganglioside	SPRi	No	2.34 ng/mL or 16 pM 100 ng/mL or 0.7 nM Only tested 100 ng/mL or 0.7 nM	Yes 10 % serum	(Malinick, Alexander S. et al., 2020)
miR-17	DNA probe	Localized SPR	Yes	1 pM	No PBS	(Miti et al., 2020)
miR-422 miR-223 miR-216 miR-23A	DNA probe	SPRi	Yes	0.55 pM 0.88 pM 1.19 pM 1.79 pM	No PBS	(Sguassero et al., 2019)
miR-145	DNA probe and fluorescent silver nanocluster	Fluorescence spectrophotometer	Yes	0.1 nM	Yes 50 % serum	(Mansourian et al., 2017)

Unidentified antibodies present in purified MS patient serum samples	Synthetic glycopeptide CSF114(Glc) with ferrocenyl moiety	Cyclic and square wave voltammetry	Yes Indirectly by excess free glycopeptide Fc-CSF114(Glc) present in solution	Not determined only reported a difference between healthy and sick samples	Yes Purified patient serum samples of 0.04 to 4 ug/mL	(Bellagha-Chenchah et al., 2015)
Unidentified antibodies present in patient serum samples	Synthetic glycopeptide CSF114(Glc)	SPR	No	Not reported only compared response between healthy and sick samples	Yes 1 % and 2 % serum	(Real-Fernández et al., 2012)

While the developed method has met the technical requirements for the routine use of blood tests for the evaluation of MS biomarkers in patient samples and even may streamline the diagnostic procedure, the observed cross reactivity suggested simple quantification by binding signals may be an oversimplified approach and could ignore potential interferences to the observed results, as is the case for the studies shown in Table 1. Therefore, an accurate detection and effective differentiation between analyte/antigen interactions would require in-depth statistical analysis.

Cross reactivity and statistical analysis

Robust statistical analysis was performed to analyze and characterize data from both SPRi sensorgrams and endpoint results. The endpoint data is the observed change in RIU of the analyte-antigen interactions after accounting for observed cross reactivity between the other biomarkers and nonspecific binding from serum. The calibration curves seen in Figure 2 are generated using the collected end point data. Further analysis was conducted using principal component analysis (PCA) and partial least squares discriminant analysis (PLS-DA), in order to characterize the data to reveal impact by specific, nonspecific, and cross reactivity interactions, yielding more thorough evaluation on antibody/ganglioside interactions than what traditional endpoint assay studies are capable of. The use of these statistical analyses gives a good assessment of the effectiveness of the ganglioside microarray's ability to screen MS biomarkers.

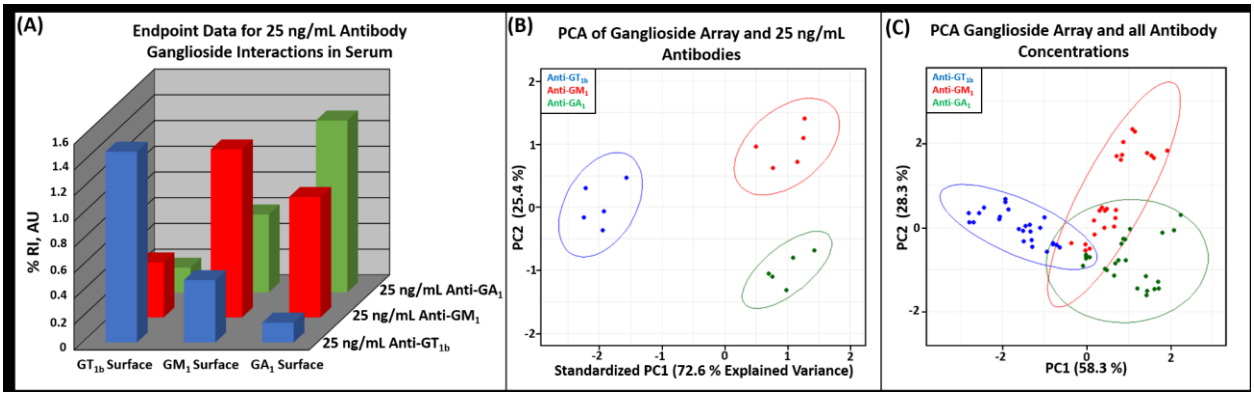

Figure 3. (A) 3D bar graph showing % RI, AU of all three antibodies interacting with the ganglioside microarray at 25 ng/mL in serum. Anti-GT_{1b} interactions (Blue), anti-GM_1 interactions in (Red), and anti-GA_1 interactions in (Green). (B) Principal component analysis (PCA) showing the ability to separate the three anti-ganglioside antibodies based on their induced response across the whole microarray at 25 ng/mL. (C) PCA of all antibody/ganglioside interactions at each concentration showing overlap of anti-GT_{1b} beginning at 10 ng/mL and at 25 ng/mL for both anti-GM_1 and anti-GA_1.

Principal component analysis was first carried out with the endpoint data for each antibody interacting with three different ganglioside surfaces individually and as an entire data set. PCA, an unsupervised statistical model with a clustering statistical algorithm that looks for linear patterns in complex data sets,(Giuliani, 2017)·(Wetzel, 2017) showed that at higher concentrations it could easily determine the specific antibody/ganglioside interactions, but was less effective in differentiating interactions at concentrations below 10 ng/mL for anti-GT_{1b} and below 25 ng/mL for anti-GM_1 and anti-GA_1. The different number of SAs on the ganglioside antigens may explain why anti-GT_{1b} antibodies could still be differentiated at 10 ng/mL, as anti-GT_{1b} specifically targets three SAs whereas anti-GM_1 and anti-GA_1 target antigenic site with one and zero SA, respectively.(Koga et al., 2001) Figure 3 shows that when all concentrations are plotted, there is a significant overlap between the antibodies at concentrations below 10 ng/mL, but at 25 ng/mL only overlap is between anti-GM_1 and anti-GA_1. This agrees well with our previous observation in 10 % serum where the majority of cross reactivity occurred between anti-GT_{1b} and anti-GM_1 or anti-GM_1 and anti-GA_1 but little between anti-GT_{1b} and anti-GA_1.(Malinick, A. S. et al., 2020) It is apparent that PCA had difficulty differentiating the antibodies at concentrations below 10 ng/mL as the measurements themselves started to show uncertainty (LODs determined around 7 ng/mL).

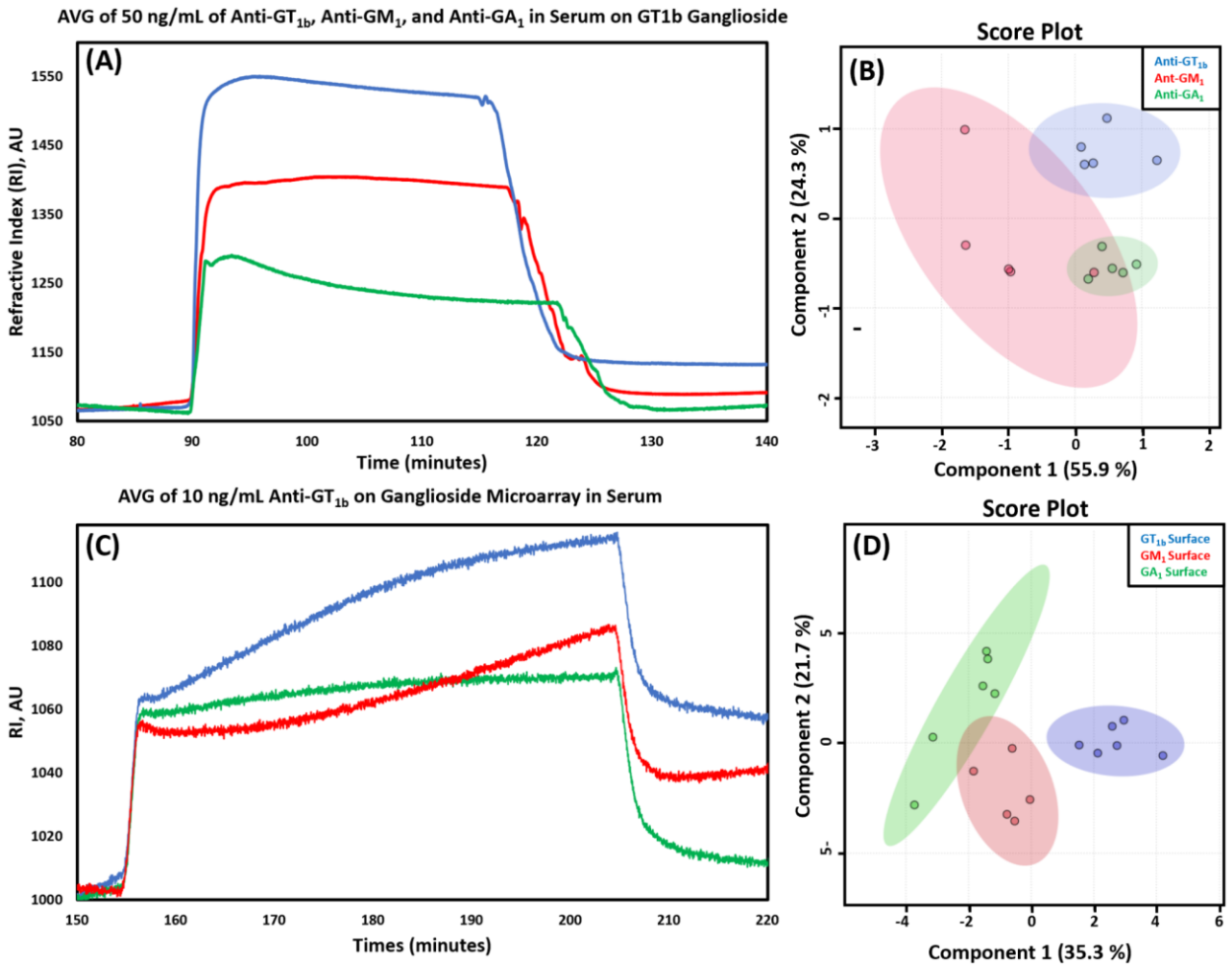

Figure 4. (A) Average of sensorgrams for binding associated regions between 50 ng/mL of the three investigated antibodies with a GT_{1b} ganglioside functionalized PFDTS surface. Anti-GT_{1b} interactions (Blue), anti-GM_1 interactions in (Red), and anti-GA_1 interactions in (Green). (B) Sample of Partial Least Squares Discriminant Analysis (PLS-DA) for all three antibodies at 50 ng/mL on a GT_{1b} ganglioside surface. (C) Average association, steady state, and dissociation regions for anti-GT_{1b} interacting with the 3 different functionalized ganglioside PFDTS surfaces. (Blue) GT_{1b} ganglioside surface, (Red) GM_1 ganglioside surface, and (Green) GA_1 ganglioside surface. (D) Sample of PLS-DA analysis of anti-GT_{1b} at 10 ng/mL classification based upon interactions with (Blue) GT_{1b} ganglioside surface, (Red) GM_1 ganglioside surface, and (Green) GA_1 ganglioside surface.

The PCA analysis with endpoint data provides a good glimpse of the interaction properties between antibodies and gangliosides, but the results are limited. Further characterization of this

complex property was carried out with kinetic interaction data from the SPRi sensorgrams. To achieve this, we utilized PLS-DA to analyze the regions associated with binding kinetics in the sensorgrams related to the antibody ganglioside interactions. PLS-DA is a supervised or classification based statistical method that looks for trends in the whole data set and makes a prediction based upon these trends to determine the relationship that one data set has to another.(Lee et al., 2018) We performed PLS-DA on the sensorgrams for 50 ng/mL of the three MS specific antibodies in serum interacting with a GT_{1b} ganglioside surface (Figure 4A) and for 10 ng/mL of anti-GT_{1b} on the 3 different ganglioside surfaces (Figure 4C). Figure 4B shows minimal overlap between anti-GT_{1b} and anti-GM_1 and between anti-GM_1 and anti-GA_1, but none between anti-GT_{1b} and anti-GA_1. The interactions observed between the three antibodies and the ganglioside surface can be attributed to anti-GA_1 not targeting SAs whereas both anti-GT_{1b} and anti-GM_1 do. In Figure 4D it is clear that 10 ng/mL anti-GT_{1b} specifically binds to the GT_{1b} ganglioside surface and there is only minor overlap between GM_1 and GA_1, while the majority of binding occurs to GT_{1b} and GM_1 ganglioside surfaces. There is no observable overlap between anti-GT_{1b} interactions with a GA_1 ganglioside surface, indicating that anti-GT_{1b} specifically targets the SA on the carbohydrates head group. PLS-DA using the kinetic interaction data appears to differentiate antibodies and ganglioside interactions more effectively than PCA did.

The promising results with PLS-DA and PCA prompted us to explore the data sets further to understand the cross reactivity between the biomarkers. Although these statistical methods are effective to reveal cross reactivity, they are limited in that only one data set was compared to another, rather than finding patterns hidden in the endpoint data, sensorgrams, and binding kinetics to predict the type of interactions that are occurring. Therefore, further statistical analysis with machine learning (ML) was performed to evaluate the SPRi raw data.

Neural Networks and k Nearest Neighbor Algorithms

ML has become increasingly relevant and present in various aspects of scientific investigation and society as a whole.(Das et al., 2015a) It appears to be only a matter of time before ML algorithms are used routinely in disease diagnostics due to its ability to handle large and complex data sets.(Cui et al., 2020) In this study we trained and tested a neural network (nnet) and

a *k*-nearest neighbor (knn) model using endpoint data for both specific and cross reactive interactions. In addition, we performed these analyses using data from the sensorgrams that are linked to association, steady state, and dissociation energies of the analyte/antigen interactions based upon the changes in time and RIU values, which gave us access to over 65,000 data points per sensorgram. By training and testing these models with the collected data, we can evaluate the effectiveness of the algorithms and the functionalized substrates for detecting and differentiating between antibody ganglioside interactions in a pseudo clinical setting. It will allow us to determine if the combination of ML to label-free sensing methodology could facilitate the general high throughput screening of antibodies/markers, which may drastically improve disease diagnosis and the monitoring of their progression.

Nnets are essentially a virtual nervous system,(Cui et al., 2020) making it an ideal ML model to use in the detection and evaluation of MS. Nnets are composed of three layers: an input, hidden, and output layer.(Volk et al., 2020) A visualization of the nnet used in our study is shown in Scheme 1C. The input layer consists of data that the user feeds into the model to train and test the success rate of the algorithm;(Shahid et al., 2019) for our study, our input layers included the time, RIU, endpoint data, and concentration depending on how we were analyzing the data. The hidden layer is the intermittent computations that occur to define patterns and investigate the data so that the algorithm can make predictions.(Cui et al., 2020) The output layer allows the user to interpret the results generated by the model, which can either be used for classification, as for the endpoint data, or a prediction, which was done for the sensorgram data.(Shahid et al., 2019) Nnets have the ability to learn by themselves and produce outputs that are not limited to the inputs originally provided to them, making them ideal for aiding in the detection and monitoring of diseases where biomarkers in one patient can vary drastically to those in another patient. Nevertheless, these new outputs would need to be verified before being included in the diagnosis criteria.

The second model used in our work was kNN. kNN is a non-parametric classification model that works by analyzing and comparing a single data point to the entirety of the data series before moving to the next data point in the series; this allows for the detection and monitoring of unique trends that other ML algorithms might overlook.(Peterson, 2009) In brief, the algorithm attempts to predict the correct class of the test data by calculating and identifying trends among a

few data points (referred to as neighbors) and defines trends amongst the entire data series or the entire neighborhood.(Cui et al., 2020) The model then compares the observed trends in the test data between individual data points, groups of data points, and the entire data series to trends observed in the training set.(Shahid et al., 2019) Unlike the nnet, all potential analyte/antigen interactions would need to be predefined for the model to accurately identify, differentiate, and predict between healthy and sick patient samples as well as which analyte/antigen interactions were most likely occurring. Given the way that the kNN algorithm operates, we were only able to reliably utilize it on the SPRi sensorgram data.

To train and determine the accuracy of the algorithms for various data sets, we implemented multiple random iterations by randomly selecting 70 % of the collected data to be used as a training set and the other 30 % to test the iteration of the model.(Shahid et al., 2019; Uçar et al., 2020; Volk et al., 2020) This allowed us to use all of the collected data to train and test the model, resulting in a more reliable algorithm than what only a portion of the data would achieve.(Shahid et al., 2019; Uçar et al., 2020) While increasing the percentage and number of training sets would undoubtedly improve the chance of the models to achieve the goal, it also carries the risk of over fitting,(Shahid et al., 2019) which is a major concern and also the reason why random iterations were utilized in this work.(Ying, 2019) The accuracies for the ML algorithms discussed here are the average of all potential random iterations conducted in the current study.

There are a few limitations to consider when using ML algorithms for this type of data analysis. One must account for all potential cross reactive interactions and nonspecific binding for the model to be considered truly reliable.(Volk et al., 2020) When potential interactions are not taken into account or considered during the training period, it is very likely that false positive and negative results will occur.(Cui et al., 2020) Nevertheless, with a model properly set-up and running, training can be completed relatively quickly as long as the data is reliable and reproducible.(Peiffer-Smadja et al., 2020)

Neural Network Data Analysis

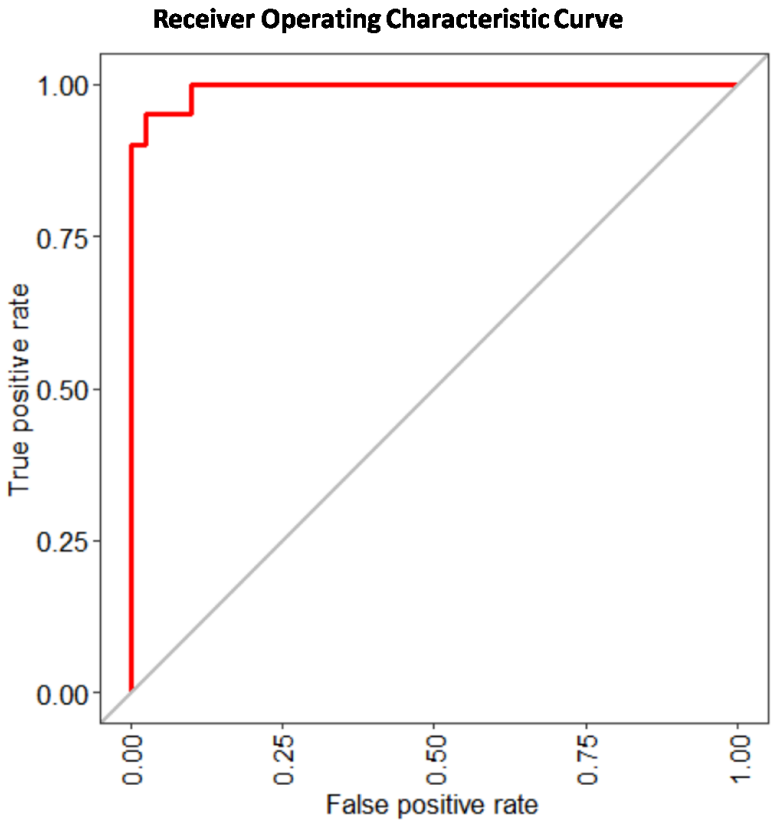

Nnet Confusion Matrix on Endpoint Data

94 % Accuracy	GA_1 Gang.	GM_1 Gang.	GT_{1b} Gang.
Anti- GA_1	21	1	0
Anti- GM_1	1	20	1
Anti- GT_{1b}	0	1	21

Figure 5. Receiver operating characteristic curve (ROC) for the analysis of the endpoint data containing all antibody/ganglioside interaction with a neural network (nnet). Below the ROC curve is a representative confusion matrix of the nnet testing data sets using random iterations, to evaluate the accuracy of the model to identify the specific analyte antigen interactions of interest.

Figure 5 shows a receiver operating curve (ROC) for the endpoint data for all antibody/ganglioside interactions at each studied concentration, which constitutes a total of 225 observations each of which contain the baseline, incubation, and post rinse cycles present in each sensorgram. An ROC depicts the reliability of the algorithm to correctly classify models at all classification thresholds based upon whether the model correctly or incorrectly identified which antibody/ganglioside interactions were observed.(Tong et al., 2018) Our ROC curve indicates that

the model has an overall accuracy of 94 %. The table shown below the ROC curve is the average of all possible random iterations that could occur, showing how accurately the model can identify for the antibody/ganglioside interactions occurring in serum. If the model was trained with all possible biomarkers associated with a disease, it could reliably differentiate and identify them based upon their specific, nonspecific, and cross reactive interactions, which would drastically improve the reliability of end point assays. We have applied the nnet to the endpoint data, which focused on using concentration and specific RIU results. In addition, we applied further analysis with the sensorgram data using both the nnet and kNN models.

The nnet modeling based on the sensorgram data was focused on three antibodies at 50 ng/mL in whole serum on a GT_{1b} ganglioside surface and anti-GT_{1b} at 10 ng/mL in serum. This dataset was selected with the consideration that GT_{1b} has the most SA groups of the three investigated gangliosides and has known cross reactivity with anti-GM_1 and little with anti-GA_1. Anti-GT_{1b} at 10 ng/mL was selected as anti-GT_{1b} had the lowest LOD (4.5 ng/mL) and LOQ (15 ng/mL) of the three investigated antibodies in whole serum and has notable cross reactivity with the GM_1 ganglioside surface and none with a GA_1 ganglioside surface as shown previously with our statistical analysis.

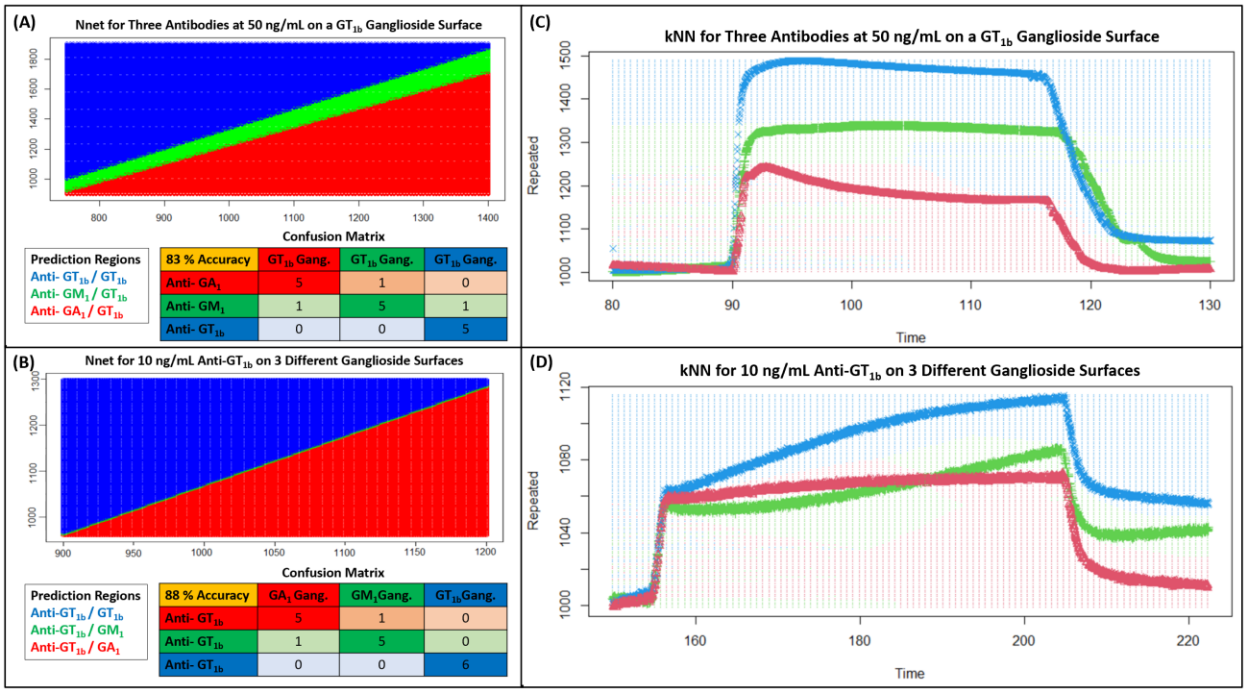

Figure 6. (A) nnet of the sensorgram for (Blue) 50 ng/mL anti-GT_{1b} on a GT_{1b} ganglioside surface, (Green) 50 ng/mL anti-GM_1 on a GT_{1b} ganglioside surface, and (Red) 50 ng/mL anti-GA_1 on a GT_{1b} ganglioside surface. (B) nnet for 10 ng/mL anti-GT_{1b} with (Blue) a GT_{1b} ganglioside surface, (Green) GM_1 ganglioside surface, and (Red) a GA_1 ganglioside surface. (C) K nearest neighbor model (kNN) depicting the binding interactions between (Red) 50 ng/mL anti-GA_1 on a GT_{1b} ganglioside surface, (Green) 50 ng/mL anti-GM_1 on a GT_{1b} ganglioside surface, and (Blue) 50 ng/mL anti-GT_{1b} on a GT_{1b} ganglioside surface. (D) KNN of 10 ng/mL anti-GT_{1b} interacting with a (Blue) GT_{1b} ganglioside surface, a (Green) GM_1 ganglioside surface, and a (Red) GA_1 ganglioside surface.

Figures 6A and 6B show the nnet plots based on the location of individual time points and their relation to specific RIU values. This is visualized as an expanded grid, depicting specific prediction regions based upon observed trends in the sensorgrams shape as well as steady state and kinetic information. A confusion matrix is shown below each expanded grid depicting the model's ability to classify which antibody/ganglioside interactions are occurring. As shown in Figures 6A and 6B, there are clearly three distinct predictive regions based upon the location of these time points and their relation to RIU values. In Figure 6A, there is a noticeable overlap between anti-GT_{1b} and anti-GM_1, as well as between anti-GM_1 and anti-GA_1, but no overlap between anti-GT_{1b} and anti-GA_1. In Figure 6B, a similar trend is observed, but the region of identification for 10 ng/mL anti-GT_{1b} interacting with a GM_1 ganglioside surface is very small compared to the dominate regions, which are the anti-GT_{1b} on a GT_{1b} ganglioside surface and anti-GT_{1b} on a GA_1 ganglioside surface. This indicates that the algorithm is able to differentiate between one antibody and three ganglioside surfaces more effectively than three antibodies and one surface. Using the sensorgram data for the three antibodies at 50 ng/mL on a GT_{1b} surface, the model has an accuracy of 83%; and for 10 ng/mL anti-GT_{1b} interacting with three different ganglioside surfaces has an accuracy of 88%. Both accuracies are lower than those of the nnet endpoint data analysis, which can be attributed to the fact that this data set has a much more complex features due to inclusion of association, steady state, and dissociation patterns.

K-Nearest Neighbor Data Analysis

The kNN algorithm was applied to the same sensorgram dataset with the same training to test ratio of 70 to 30 %. As seen in Figures 6C and 6D, the most likely paths to occur based upon the specific analyte/antigen interactions from the training datasets are the solid lines. The colored individual data points that surround the predicted paths are the cluster regions where specific analyte/antigen interactions are most likely to occur. Notable confusion can be observed in both Figures 6C and 6D in relation to the model's clustering analysis capabilities in regards to regions related to association and dissociation interactions. However, in regions related to the steady state and post rinse cycles, the algorithm is highly successful. Even with these regions of high confusion, the model produced high accuracy rates above 90 %. Specifically, we obtained 94 % accuracy for 50 ng/mL of three antibodies on a GT_{1b} ganglioside surface and 96 % for 10 ng/mL anti-GT_{1b} interacting with three different ganglioside surfaces. The higher accuracy for differentiating between ganglioside surfaces instead of antibodies agrees well with the findings of the nnet and PLS-DA, as discussed previously.

The high accuracy observed for the kNN model in comparison to the nnet algorithm can be attributed to the different approach by which the algorithms analyze the data series.(Peterson, 2009; Shahid et al., 2019) Both algorithms identify that there is a higher probability of experiencing confusion between anti-GM_1 with the other two antibodies due to higher cross reactivity. In addition, they agree on no confusion between anti-GT_{1b} and anti-GA_1. Both models also show that differentiating between one antibody and three ganglioside surfaces is much more reliable than differentiating between three antibodies and one ganglioside surface. These findings agree well with the statistical analysis previously discussed to characterize the microarrays ability to differentiate between analyte/antigen interactions. It also shows that these models are capable of identifying an antibody that is interacting specifically with a ganglioside surface based upon endpoint data, association, steady state, and dissociation kinetics.

Using the sensorgram dataset in combination with the endpoint data appears to be more effective than relying on either one separately for disease biomarker characterization. The combination allows for a more comprehensive review of the observed interactions, and also for faster identification of abnormalities that individual ML algorithms may miss. This is critical to the analysis of patient samples, where there is a high likelihood that unforeseen interactions could have occurred that were not accounted for in the training series, such as those from patient's therapeutics/drugs and other disease biomarkers that are not affiliated with MS.(Peiffer-Smadja et

al., 2020) Relying on endpoint data alone may cause higher than expected false positive or negative results due to these unaccounted interactions. We demonstrated that utilizing binding kinetic interactions with the endpoint data, the unaccounted interactions could be more easily identified and then corrected by the models. The findings of this study have the potential to drastically improve label free detection methods as well as the reliability of screening many biomarkers simultaneously.

Conclusion

In this work, we have shown that SPRi microarray biochips in combination with robust statistical algorithms are capable of detecting, identifying, and differentiating antibody/ganglioside interactions in whole serum samples. The work addressed a major concern of using antibodies for the diagnosis of MS in a clinical setting, which is the high individual heterogeneity in patients and the widely varied concentration range. We demonstrated that developing a detection scheme allowing a range of antibodies measured with multiplexed capability, under identical assay conditions, and being able to account for cross reactivity and nonspecific interactions is critical. Using the PFDTS surface, the microarray can be easily extended to include more antigens desired, and the hydrophobic regions will minimize the interferes from the background proteins. This is ideal for glycolipids and sphingomyelins, which are the major components of the myelin sheath. All three targeted antibodies were detectable and quantifiable within biologically relevant concentrations between 3 ng/mL to 25 ng/mL. The statistical analysis and machine learning algorithms implemented in this study allowed for the observation and evaluation of unique trends and features between the antibodies and antigens, which allowed us to conduct a more intense evaluation and gain a broader understanding than what traditional assays can achieve. The method demonstrated here may improve patient-specific evaluation of MS biomarkers, and find use in helping understand the disease progression. As can be seen from these results, robust data analysis protocols are integral for future disease detection studies based on the complexity of biological interactions.

Acknowledgements:

The authors acknowledge supports from the National Institute of Health (R21 AI140461) and NSF (CHE-2109042). A.S.L. was supported by an NIEHS T32 training grant (T32-ES018827).

References:

Abbas, A., Linman, M.J., Cheng, Q., 2011. Patterned resonance plasmonic microarrays for high-performance SPR imaging. Anal Chem 83(8), 3147-3152.

Bellagha-Chenchah, W., Sella, C., Fernandez, F.R., Peroni, E., Lolli, F., Amatore, C., Thouin, L., Papini, A., 2015. Interactions between human antibodies and synthetic conformational peptide epitopes: innovative approach for electrochemical detection of biomarkers of multiple sclerosis at platinum electrodes. Electrochimica Acta 176, 1239-1247.

Brownlee, W.J., Hardy, T.A., Fazekas, F., Miller, D.H., 2017. Diagnosis of multiple sclerosis: progress and challenges. Lancet 389(10076), 1336-1346.

Broza, Y.Y., Zhou, X., Yuan, M., Qu, D., Zheng, Y., Vishinkin, R., Khatib, M., Wu, W., Haick, H., 2019. Disease Detection with Molecular Biomarkers: From Chemistry of Body Fluids to Nature-Inspired Chemical Sensors. Chem Rev 119(22), 11761-11817.

Cawley, J.L., Jordan, L.R., Wittenberg, N.J., 2021. Detection and Characterization of Vesicular Gangliosides Binding to Myelin-Associated Glycoprotein on Supported Lipid Bilayers. Anal Chem 93(2), 1185-1192.

Clark, L.F., Kodadek, T.J.A.c.n., 2016. The immune system and neuroinflammation as potential sources of blood-based biomarkers for Alzheimer's disease, Parkinson's disease, and Huntington's disease. ACS chemical neuroscience 7(5), 520-527.

Costerus, J.M., Brouwer, M.C., van de Beek, D., 2018. Technological advances and changing indications for lumbar puncture in neurological disorders. Lancet Neurol 17(3), 268-278.

Cui, F., Yue, Y., Zhang, Y., Zhang, Z., Zhou, H.S., 2020. Advancing Biosensors with Machine Learning. ACS Sens 5(11), 3346-3364.

D'Agata, R., Bellassai, N., Jungbluth, V., Spoto, G.J.P., 2021. Recent Advances in Antifouling Materials for Surface Plasmon Resonance Biosensing in Clinical Diagnostics and Food Safety. Polymers 13(12), 1929.

Damodaran, V.B., Murthy, N.S., 2016. Bio-inspired strategies for designing antifouling biomaterials. Biomater Res 20(1), 18.

Das, S., Dey, A., Pal, A., Roy, N., 2015a. Applications of artificial intelligence in machine learning: review and prospect. International Journal of Computer Applications 115(9).

Das, S., Dey, A., Pal, A., Roy, N.J.I.J.o.C.A., 2015b. Applications of artificial intelligence in machine learning: review and prospect. International Journal of Computer Applications 115(9).

Derkus, B., Bozkurt, P.A., Tulu, M., Emregul, K.C., Yucesan, C., Emregul, E., 2017. Simultaneous quantification of Myelin Basic Protein and Tau proteins in cerebrospinal fluid and serum of Multiple Sclerosis patients using nanoimmunosensor. Biosensors and Bioelectronics 89, 781-788.

Ghasemi, N., Razavi, S., Nikzad, E., 2017. Multiple Sclerosis: Pathogenesis, Symptoms, Diagnoses and Cell-Based Therapy. Cell J 19(1), 1-10.

Giuliani, A., 2017. The application of principal component analysis to drug discovery and biomedical data. Drug Discov Today 22(7), 1069-1076.

Graner, M., Pointon, T., Manton, S., Green, M., Dennison, K., Davis, M., Braiotta, G., Craft, J., Edwards, T., Polonsky, B.J.P.o., 2020. Oligoclonal IgG antibodies in multiple sclerosis target patient-specific peptides. PloS one 15(2), e0228883.

Häusser-Kinzel, S., Weber, M.S.J.F.i.i., 2019. The role of B cells and antibodies in multiple sclerosis, neuromyelitis optica, and related disorders. Frontiers in immunology 10, 201.

Höftberger, R., Guo, Y., Flanagan, E.P., Lopez-Chiriboga, A.S., Endmayr, V., Hochmeister, S., Joldic, D., Pittock, S.J., Tillema, J.M., Gorman, M.J.A.n., 2020. The pathology of central nervous system inflammatory demyelinating disease accompanying myelin oligodendrocyte glycoprotein autoantibody. Acta neuropathologica, 1-18.

Hogan, E.L., Podbielska, M., O'Keeffe, J., 2013. Implications of lymphocyte anergy to glycolipids in multiple sclerosis (MS): iNKT cells may mediate the MS infectious trigger. Journal of clinical & cellular immunology 4(3).
Ivanova, M., Zakharova, M.J.H.P., 2017. Antibodies against myelin lipids in multiple sclerosis. Human Physiology 43(8), 875-880.
Kappler, K., Hennet, T., 2020. Emergence and significance of carbohydrate-specific antibodies. Genes Immun 21(4), 224-239.
Koga, M., Tatsumoto, M., Yuki, N., Hirata, K., 2001. Range of cross reactivity of anti-GM1 IgG antibody in Guillain-Barré syndrome. Journal of Neurology, Neurosurgery Psychiatry 71(1), 123-124.
Kuerten, S., Lanz, T.V., Lingampalli, N., Lahey, L.J., Kleinschnitz, C., Mäurer, M., Schroeter, M., Braune, S., Ziemssen, T., Ho, P.P.J.P.o.t.N.A.o.S., 2020. Autoantibodies against central nervous system antigens in a subset of B cell–dominant multiple sclerosis patients. Proceedings of the National Academy of Sciences 117(35), 21512-21518.
Lambert, A., Yang, Z., Cheng, W., Lu, Z., Liu, Y., Cheng, Q., 2018. Ultrasensitive Detection of Bacterial Protein Toxins on Patterned Microarray via Surface Plasmon Resonance Imaging with Signal Amplification by Conjugate Nanoparticle Clusters. ACS Sens 3(9), 1639-1646.
Lambert, A.S., Valiulis, S.N., Malinick, A.S., Tanabe, I., Cheng, Q., 2020. Plasmonic Biosensing with Aluminum Thin Films under the Kretschmann Configuration. Anal Chem 92(13), 8654-8659.
Lee, L.C., Liong, C.Y., Jemain, A.A., 2018. Partial least squares-discriminant analysis (PLS-DA) for classification of high-dimensional (HD) data: a review of contemporary practice strategies and knowledge gaps. Analyst 143(15), 3526-3539.
Lycke, J., Zetterberg, H., 2017. The role of blood and CSF biomarkers in the evaluation of new treatments against multiple sclerosis. Expert Rev Clin Immunol 13(12), 1143-1153.
Malinick, A.S., Lambert, A.S., Stuart, D.D., Li, B., Puente, E., Cheng, Q., 2020. Detection of Multiple Sclerosis Biomarkers in Serum by Ganglioside Microarrays and Surface Plasmon Resonance Imaging. ACS Sensors 5(11), 3617-3626.
Malinick, A.S., Lambert, A.S., Stuart, D.D., Li, B., Puente, E., Cheng, Q., 2020. Detection of Multiple Sclerosis Biomarkers in Serum by Ganglioside Microarrays and Surface Plasmon Resonance Imaging. ACS Sens 5(11), 3617-3626.
Mansourian, N., Rahaie, M., Hosseini, M., 2017. A Nanobiosensor based on fluorescent DNA-hosted silver nanocluster and HCR amplification for detection of MicroRNA involved in progression of multiple sclerosis. Journal of fluorescence 27(5), 1679-1685.
Masson, J.F., 2017. Surface Plasmon Resonance Clinical Biosensors for Medical Diagnostics. ACS Sens 2(1), 16-30.
Mescheriakova, J.Y., Wong, Y.Y.M., Runia, T.F., Jafari, N., Samijn, J.P., de Beukelaar, J.W., Wokke, B.H., Siepman, T.A., Hintzen, R.Q.J.J.n., 2018. Application of the 2017 revised McDonald criteria for multiple sclerosis to patients with a typical clinically isolated syndrome. JAMA neurology 75(11), 1392-1398.
Miti, A., Thamm, S., Müller, P., Csáki, A., Fritzsche, W., Zuccheri, G., 2020. A miRNA biosensor based on localized surface plasmon resonance enhanced by surface-bound hybridization chain reaction. Biosensors and Bioelectronics 167, 112465.
Mizutani, K., Oka, N., Kusunoki, S., Kaji, R., Mezaki, T., Akiguchi, I., Shibasaki, H.J.J.o.t.n.s., 2001. Sensorimotor demyelinating neuropathy with IgM antibody against gangliosides GD1a, GT1b and GM3. Journal of the neurological sciences 188(1-2), 9-11.
Nair, S., Gomez-Cruz, J., Manjarrez-Hernandez, A., Ascanio, G., Sabat, R.G., Escobedo, C., 2020. Rapid label-free detection of intact pathogenic bacteria in situ via surface plasmon resonance imaging enabled by crossed surface relief gratings. Analyst 145(6), 2133-2142.
Nowack, L., Teschers, C.S., Albrecht, S., Gilmour, R., 2021. Oligodendroglial glycolipids in (Re)myelination: implications for multiple sclerosis research. Nat Prod Rep 38(5), 890-904.

Peiffer-Smadja, N., Rawson, T.M., Ahmad, R., Buchard, A., Georgiou, P., Lescure, F.-X., Birgand, G., Holmes, A.H., 2020. Machine learning for clinical decision support in infectious diseases: a narrative review of current applications. Clinical Microbiology Infection 26(5), 584-595.
Pender, M.P., Csurhes, P.A., Wolfe, N.P., Hooper, K.D., Good, M.F., McCombe, P.A., Greer, J.M., 2003. Increased circulating T cell reactivity to GM3 and GQ1b gangliosides in primary progressive multiple sclerosis. Journal of clinical neuroscience 10(1), 63-66.
Peterson, L.E., 2009. K-nearest neighbor. Scholarpedia 4(2), 1883.
Real-Fernández, F., Passalacqua, I., Peroni, E., Chelli, M., Lolli, F., Papini, A.M., Rovero, P., 2012. Glycopeptide-based antibody detection in multiple sclerosis by surface plasmon resonance. Sensors 12(5), 5596-5607.
Rikkert, L.G., de Rond, L., van Dam, A., van Leeuwen, T.G., Coumans, F.A.W., de Reijke, T.M., Terstappen, L., Nieuwland, R., 2020. Detection of extracellular vesicles in plasma and urine of prostate cancer patients by flow cytometry and surface plasmon resonance imaging. PLoS One 15(6), e0233443.
Schnaar, R.L., 2010. Brain gangliosides in axon–myelin stability and axon regeneration. FEBS letters 584(9), 1741-1747.
Sguassero, A., Artiga, Á., Morasso, C., Jimenez, R.R., Rapún, R.M., Mancuso, R., Agostini, S., Hernis, A., Abols, A., Linē, A., 2019. A simple and universal enzyme-free approach for the detection of multiple microRNAs using a single nanostructured enhancer of surface plasmon resonance imaging. Analytical bioanalytical chemistry 411(9), 1873-1885.
Shahid, N., Rappon, T., Berta, W., 2019. Applications of artificial neural networks in health care organizational decision-making: A scoping review. PLoS One 14(2), e0212356.
Sharafeldin, M., Davis, J.J., 2021. Point of Care Sensors for Infectious Pathogens. Anal Chem 93(1), 184-197.
Shedko, E., Tyumentseva, M.J.N., Physiology, B., 2020. Molecular Biomarkers in the Cerebrospinal Fluid in Multiple Sclerosis. Neuroscience and Behavioral Physiology 50(5), 527-533.
Tong, X., Feng, Y., Li, J.J., 2018. Neyman-Pearson classification algorithms and NP receiver operating characteristics. Sci Adv 4(2), eaao1659.
Uçar, M.K., Nour, M., Sindi, H., Polat, K., 2020. The effect of training and testing process on machine learning in biomedical datasets. Mathematical Problems in Engineering 2020.
Volk, M.J., Lourentzou, I., Mishra, S., Vo, L.T., Zhai, C., Zhao, H., 2020. Biosystems Design by Machine Learning. ACS Synth Biol 9(7), 1514-1533.
Wanleenuwat, P., Iwanowski, P., 2019. Role of B cells and antibodies in multiple sclerosis. Mult Scler Relat Disord 36, 101416.
Wetzel, S.J., 2017. Unsupervised learning of phase transitions: From principal component analysis to variational autoencoders. Phys Rev E 96(2-1), 022140.
Wilkop, T., Wang, Z., Cheng, Q., 2004. Analysis of micro-contact printed protein patterns by SPR imaging with a LED light source. Langmuir 20(25), 11141-11148.
Wu, W., Yu, X., Wu, J., Wu, T., Fan, Y., Chen, W., Zhao, M., Wu, H., Li, X., Ding, S.J.B., Bioelectronics, 2021. Surface plasmon resonance imaging-based biosensor for multiplex and ultrasensitive detection of NSCLC-associated exosomal miRNAs using DNA programmed heterostructure of Au-on-Ag. Biosensors and Bioelectronics 175, 112835.
Yang, M., Huang, J., Fan, J., Du, J., Pu, K., Peng, X., 2020. Chemiluminescence for bioimaging and therapeutics: recent advances and challenges. Chem Soc Rev 49(19), 6800-6815.
Ying, X., 2019. An overview of overfitting and its solutions, Journal of Physics: Conference Series. IOP Publishing, p. 022022.
Ziemssen, T., Akgun, K., Bruck, W., 2019. Molecular biomarkers in multiple sclerosis. J Neuroinflammation 16(1), 272.